New Phytologist

How do cold-sensitive species endure ice ages? Phylogeographic and paleodistribution models of postglacial range expansion of the mesothermic drought-tolerant conifer *Austrocedrus chilensis*

Cintia P. Souto[1], Thomas Kitzberger[1], Marina P. Arbetman[1,2] and Andrea C. Premoli[1]

[1]Laboratorio Ecotono-INIBIOMA-CONICET, Universidad Nacional del Comahue, Quintral 1250, Bariloche 8400, Río Negro, Argentina; [2]Universidad Nacional de Río Negro, Sede Andina, Bariloche 8400, Río Negro, Argentina

Author for correspondence:
Cintia P. Souto
Tel: +54 2944428505 ext. 158
Email: cintiap.souto@gmail.com

Received: *21 November 2014*
Accepted: *7 May 2015*

New Phytologist (2015) **208:** 960–972
doi: 10.1111/nph.13508

Key words: glaciations, Last Glacial Maximum (LGM) refugia, microsatellite markers, MIGRATE, species distribution models (SDMs).

Summary

- In view of global climate change, it is important to understand the responses of tree species to climate changes in the past. Combinations of phylogeographic analysis of genetic evidence, coupled with species distribution models (SDMs), are improving our understanding on this subject.
- We combined SDMs and microsatellite data from populations of the entire range of *Austrocedrus chilensis*, a dominant mesotherm (cold-sensitive) conifer of dryland forests of the southern Andes, to test the hypothesis of long-distance postglacial migration from northern and warmer refugia at the Last Glacial Maximum (LGM).
- The SDM indicated suitable conditions for *Austrocedrus* in northern Chile (western) at the LGM and largely unsuitable conditions in Argentina (eastern). Population genetic diversity and effective population sizes within populations decreased southward along the Andes, consistent with the hypothesis of long-distance dispersal from a northern refugium.
- Results support the hypothesis of one (or a few) warmer (low latitude) refugia in Chile for *Austrocedrus*. On balance, the evidence suggests that in contrast to cold-tolerant tree taxa with the capacity to fast-track postglacial warming thanks to local refugia, cold-sensitive species might have undergone long-distance range expansion, lagging behind progressive climate change throughout the Holocene.

Introduction

In the face of changing climate, plant species can retract and endure locally, and recolonize afterwards, but they can alternatively undergo massive range shifts, both before and after such periods. At least those have been the observed alternative responses of plant species to past climate changes. Understanding the adaptive implications of such alternative responses is key to our assessment of any species' potential to survive past, impending or future climate changes (Pearson *et al.*, 2006). Postglacial Holocene warming provides the most recent episode of species' responses to changing environmental conditions. Over recent decades a wealth of paleoecological evidence has shown extremely rapid recolonization rates (in excess of 1 km yr^{-1}), suggesting facile dispersal and malleable demography (Petit *et al.*, 2008). New evidence suggests slower migration rates (< 0.1 km yr^{-1}) and lower species capacities to track future climate change (McLachlan *et al.*, 2005).

Past demographic events leave long-lasting imprints on modern-day genetic patterns that might help to solve some of the ambiguities of pollen signatures (Hu *et al.*, 2009; Hampe *et al.*, 2013). Range expansion, typically involving a succession of founder events, leaves a signature of declining genetic diversity with increasing distance from the origin of expansion (Slatkin & Excoffier, 2012). In addition, range expansions tend to produce gradients in allele frequencies along the axis of the expansion (Slatkin & Excoffier, 2012); creating clinal patterns (Débarre *et al.*, 2013). Furthermore, species distribution models (SDMs) provide valuable information on potential range retractions and expansions under different climatic circumstances (Nogués-Bravo, 2009). Combinations of paleoecological and phylogeographic analyses of genetic evidence, coupled with SDMs, are improving our understanding of how species responded to past climatic changes (Ortego *et al.*, 2012; Gavin *et al.*, 2014).

Despite increased awareness that species may have survived in small patches of environmentally favorable microclimate at the Last Glacial Maximum (LGM, 21 000 yr before present, kyr BP), even under harsh conditions at higher latitudes (Markgraf *et al.*, 1995), it is clear that such local refugia cannot be viewed as generally available to plants with different tolerances to climatic conditions. Conversely, if recolonization rates were slow, and species retreated to single distant refugia without leaving scattered

populations, time lags are expected for recolonization, subsequent to later environmental amelioration (Normand *et al.*, 2011). Such time lags imply that taxa may remain for extended periods of time in a state of nonequilibrium with current climate (Birks, 1981; Svenning & Skov, 2004, 2007). It becomes important to distinguish between climate-responsive (fast-track) taxa, capable of surviving in small local populations that have responded rapidly to amelioration, and dispersal-limited (slow-track) taxa that have retreated to LGM areas (at lower latitudes), and which have experienced extensive postglacial recolonization histories.

A suite of genetic studies in temperate South America suggest that relatively microthermic (cold-tolerant) forest dominant woody genera (*Nothofagus*, *Araucaria*, *Fitzroya*, *Pilgerodendron*, *Podocarpus*, *Embothrium*) were able to survive glacial periods locally in multiple ice-free, high-latitude refugia (*sensu* Premoli, 1998) as isolated populations (Premoli, 1997; Premoli *et al.*, 2000, 2002; Souto & Premoli, 2008; Mathiasen & Premoli, 2010; Quiroga & Premoli, 2010; Vidal-Russell *et al.*, 2011; Acosta *et al.*, 2014). In addition, palynological evidence from formerly glaciated areas shows early reoccupation, indicated by pollen increases for these taxa, shortly after deglaciation (Markgraf *et al.*, 2013; Supporting Information Table S1).

The location of glacial refugia and the postglacial migrational history of the mesothermic – drought-tolerant – *Austrocedrus chilensis* (hereafter *Austrocedrus*) is less clear. Biogeographic patterns of isozyme (Pastorino & Gallo, 2002) and microsatellite variation (Arana *et al.*, 2010), proposed that during glacial times the species may have retracted eastwards to multiple marginal populations toward the Patagonian steppe (outside ice-covered areas). These studies, however, assessed nuclear genetic variation for populations only along the eastern (Argentine) range, lacking population samples from west of the Andes in Chile. Scenarios of eastern populations acting as local sources of fast-track postglacial colonization into extant western mesic populations do not fully match the pollen record of the region (Table S1). In particular, records described so far show a hiatus of Cupressaceae pollen from the late postglacial, followed later by a sudden mid-Holocene pulse. Such a time lag seems incompatible with a fast-track expansion of *Austrocedrus* from nearby refugia. However, pollen records do not always discriminate between small remnant populations suggesting local persistence (sometimes referred to as 'cryptic refugia'), and deposition of pollen that might have arrived from distant sources. A possible complication with using the pollen record, however, is that *Austrocedrus* has the same pollen type as two other genera of the Cupressaceae, *Fitzroya cupressoides* and *Pilgerodendron uviferum* (Markgraf *et al.*, 2013), both water-tolerant microtherms (cold-tolerant). Both species seem to have persisted in multiple east-Andean refugia during glacial times, compatible both with their continuous pollen records (Table S1) and available molecular genotypes (Allnutt *et al.*, 1999, 2003; Premoli *et al.*, 2000, 2001). So, typical early postglacial Cupreassaceae pollen peaks used as an additional argument to support multiple eastern refugia hypothesis of *Austrocedrus* may possibly reflect expansion from local refugia by *Fitzroya* and *Pilgerodendron*.

In order to resolve the uncertainties about postglacial recolonization pattern for *Austrocedrus*, we constructed an SDM and combined that with a species-wide analysis of nuclear microsatellite markers. Our objectives were to: analyze range expansion, divergence time and migration estimates, based on coalescent models, and construct a credible scenario of glacial retraction/postglacial recolonization for *Austrocedrus*. We also elaborate upon the past potential distribution of *Austrocedrus* and a network of existing pollen records to discuss emerging hypotheses and predictions for the future of this species, under current and projected climate change.

Materials and Methods

Austrocedrus chilensis (D. Don) Florin & Boutelje is one of the three monotypic genera of the Patagonian conifer family Cupressaceae. *Austrocedrus* is a dioecious (but occasionally diclinous monoecious) tree species. The pollen has limited wind dispersal (Markgraf *et al.*, 1981) and 95% of winged seeds disperse < 43 m from a given forest boundary (Kitzberger, 1994). *Austrocedrus* has a naturally fragmented latitudinal range along the Andean cordillera. West of the Andes in Chile, *Austrocedrus* has a restricted range covering < 45 000 ha (CONAF *et al.*, 1999), and it occurs in small, isolated populations as far north as 32°39′S, but in relatively larger populations between 34°45′ and 38°S (Veblen *et al.*, 1995) in both the Andes and the Coastal Cordillera. Further South, it reappears sporadically, at 40°30′S (Veblen & Schlegel, 1982) and at 43°36′S, on the western outskirts of more a continuous forest in Argentina, where the species occurs as denser but naturally fragmented stands (Dezzotti & Sancholuz, 1991), with a total area of *c.* 13.6 Mha (Bran *et al.*, 2002). On the eastern slopes of the Argentinean Andes, the northernmost zone of occupation ranges from 37°07′S to 39°30′S, mostly as scattered populations. It extends southward to 43°44′S (Bran *et al.*, 2002) as a 60–80-km-wide strip of increasingly larger populations, with a more continuous distribution towards the south (Seibert, 1972). *Austrocedrus* is now listed as Vulnerable, and is at high risk of extinction (IUCN, 2014).

Austrocedrus experiences Mediterranean-type climates, with annual rainfall between 500 and 1700 mm and up to 6 months of summer water deficit, reflecting its drought tolerance (Veblen *et al.*, 1995). In areas of higher rainfall *Austrocedrus* is outcompeted by *Nothofagus* species, except in xeric microsites of low productivity, such as rock outcrops. *Austrocedrus* occupies mild topographic positions such as northerly aspects, and it is virtually absent from cold-air drainage valley bottoms, as it is intolerant of cold frost-prone conditions, making it a species with relatively mesothermal requirements (Donoso, 1982).

Sampling

Sampling covered most of the range of *Austrocedrus* in Chile and Argentina, between 37°S and 43°S (Fig. 1; Table S2). Samples were collected from 42 populations, selecting 10 random individuals per population, wherever available (Table S2). Each sample consisted of 20-cm-long terminal twigs of fresh leaf tissue

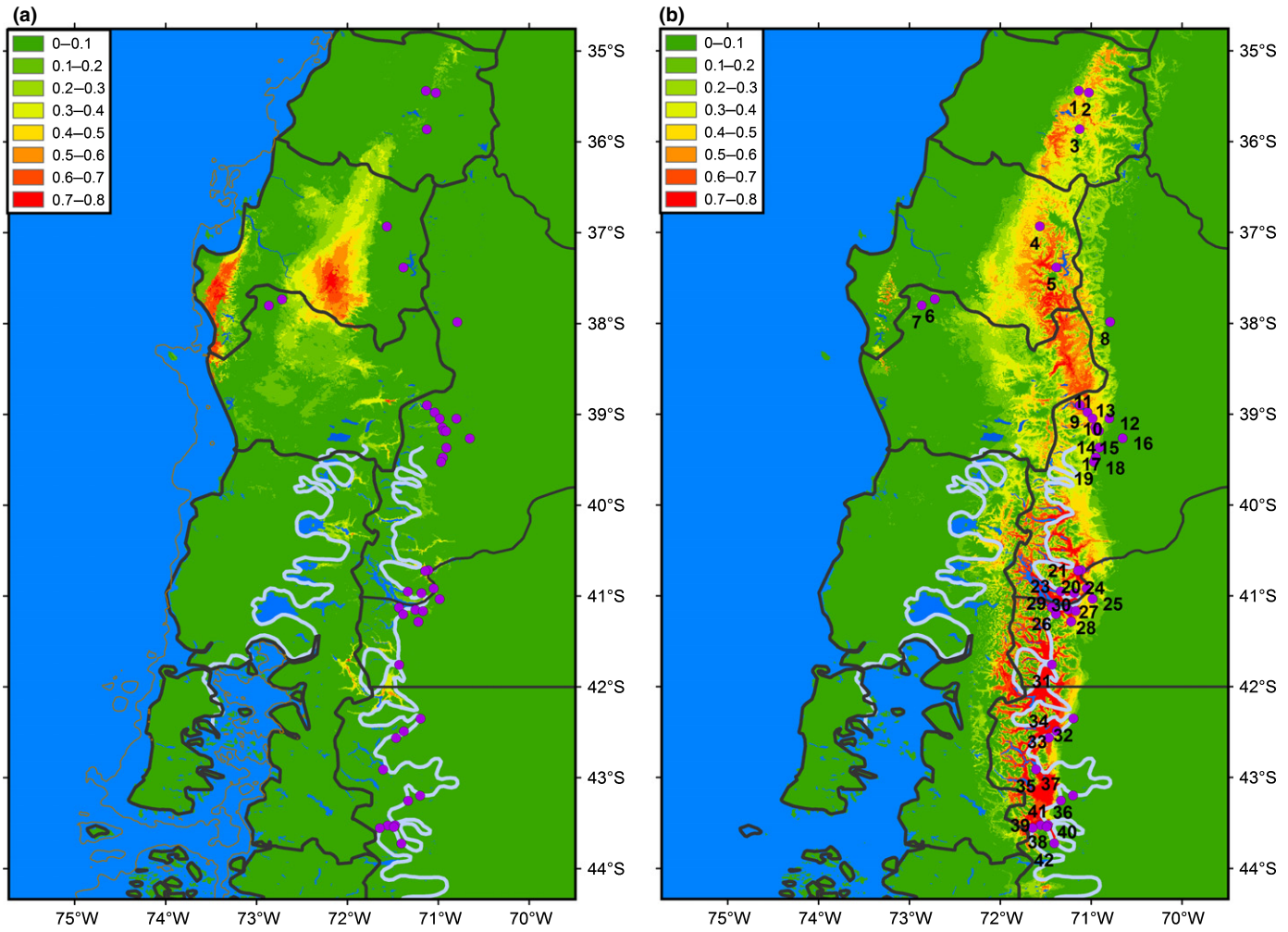

Fig. 1 Species distribution models (SDMs) results: warmer colors represent areas of higher suitability (in red) under (a) Last Glacial Maximum (LGM) and (b) current climatic conditions along the *Austrocedrus* range. Part (a) includes a bathymetric line and ice limit (LGM coastline from Smith & Sandwell, 1997).

collected from adult trees. Each population was GPS located. The 42 populations were grouped into four, relatively disjunct regions, which had already been shown to have distinct allozyme divergence (Souto *et al.*, 2012): Chile (Ch, populations 1–7) from the Coastal and Andean Cordillera; northern Argentina (Ar_N, populations 8–19, 37–39°S latitude), characterized by dry climatic conditions and low vegetation cover; central Argentina (Ar_C, populations 20–30, 40–41°S), where the gradient of continuous to fragmented forest is more evident at the eastern margin; and southern Argentina (Ar_S, populations 31–42, 41–43°S), with relatively high precipitation and large forest patches.

DNA extraction and microsatellite genotyping

DNA was extracted using a modified ATMAB protocol (Doyle, 1990; Dumolin *et al.*, 1995). Having tried 21 cpDNA primers, all of them invariant along the species range, we used five polymorphic nuclear microsatellite makers to genotype *Austrocedrus* trees, developed specifically for this study. A setup for PCR conditions was performed for each primer pair (Methods S1).

SDM

Species distribution modeling was carried out to determine a suitable bioclimatic envelope for *Austrocedrus* during the LGM using the maximum entropy approach implemented in the MaxEnt software package (v3.3.3; Phillips *et al.*, 2006) (Fig. S1). Comprehensive current species occurrence data were obtained from the Valdivian Ecoregion forest map that includes the entire species range, based on a complete aerial photography/remote sensing survey (INTA *et al.*, 1999), ensuring minimal bias in the training set. Although the number of training points is large, we did not subsample the dataset, because the distribution of the species is relatively uniform across the study area (in the form of small patches), as opposed to highly skewed patch size distribution, so nonrandom sampling effort/effects are unlikely.

We clipped the present-day WorldClim dataset (1950–2000), at 30-s resolution, comprising 19 bioclimatic summaries of means and variation in temperature and precipitation (Hijmans *et al.*, 2005); to the species' approximate current distribution. To create LGM climate layers for projecting the

bioclimatic envelope, we used LGM bioclimatic inputs at 2.5-min resolution that were drawn from the 21 kyr BP simulations using the Community Climate System Model (NCAR-CCSM; Collins *et al.*, 2006) (see Methods S2 for complete MaxEnt settings).

Genetic variation

We tested for linkage equilibrium between each pair of loci based on 200 permutations in Fstat v2.9.1 (Goudet, 2000). Also, we checked for large allele drop out and presence of nonamplifying (null) alleles with Micro-Checker v2.23 (van Oosterhout *et al.*, 2004). The extent of microsatellite variation for single populations and geographic groups was described by standard gene diversity measures, using GenAlEx 6.5 (Peakall & Smouse, 2012). Calculated parameters were: mean number of alleles per locus (A), mean effective number of alleles (A_E), percentage of polymorphic loci s.s. ($P_{\%}$); observed (H_O) and expected (H_E) heterozygosity, mean number of private alleles per locus (P_A) and total number of private alleles (P_T). Shared allele frequency (SAF) was calculated averaging within-population allele frequencies of the alleles present in all regions, that is those that are not private. We then correlated these parameter estimates with latitude, to test for clines in genetic diversity under the range expansion hypothesis. Genetic diversity was analyzed at the regional level clustering populations according to their location in four regions (Tables 1, S2). Mean and standard error of each genetic diversity parameter were calculated for each region (Ch, Ar_N, Ar_C, Ar_S), and the differences in these parameters between regions were analyzed using Fstat v2.9.1 (Goudet, 2000), reporting the one-sided P-values obtained after 9999 permutations. Differences between regions were analyzed by performing separate AMOVAs using GenAlEx with a permutational jackknifing procedure, to determine pairwise significant differences ($P < 0.05$) among regions (Peakall & Smouse, 2012).

Genetic inbreeding, divergence and structure

We estimated within-population inbreeding (F_{IS}) and divergence within and among regions with F_{ST} and R_{ST} over all samples, following Rousset (1996) and Goodman (1997), as the fraction of total genetic variance attributable to differences among populations. The mean and 95% confidence intervals (CI) were calculated by jackknifing and bootstrapping over polymorphic loci, respectively, using FSTAT v2.9.1 (Goudet, 2000). To test for spatial genetic structure (SGS) in refugial and recolonized areas, we generated a matrix of pairwise F_{ST} values along with a matrix of pairwise geographical distances (km) for Chilean and Argentine populations, respectively, under the expectation of stronger regional SGS in refugial than in recolonized areas (Slatkin, 1993). This was analysed by Mantel tests for each area (9999 permutations) using GenAlEx 6.5 (Peakall & Smouse, 2006, 2012) and differences in slopes were tested in Statistica 7 (StatSoft Inc., Tulsa, OK, USA).

We tested the genetic clustering of *Austrocedrus* individuals using a Bayesian approach implemented in Structure v2.1 (Pritchard *et al.*, 2000). We conducted independent runs to assign individual *Austrocedrus* genotypes to different number of populations (K) ranging from 1 to 10. We report Structure detail methods, parameter settings, graphic results and values as suggested by Gilbert *et al.* (2012) (Methods S3). As a validation approach to the Bayesian clustering, we conducted a PCoA in GenAlEx 6.5, via a covariance matrix with standardized genetic distances.

Effective population size, migration and coalescence time

In order to estimate population size and migration parameters, microsatellite data were analyzed using the program Migrate-N v3.5.1 (Beerli, 2002). We inferred the population parameters, migration rates among regions and associated thetas, using a Bayesian approach and the Brownian motion mutation model, based on coalescent theory (Beerli & Palczewski, 2010). Migrate-n was run using the Bayesian mode with a Metropolis-coupled heating scheme, using one cold and three heated chains; each of four chains was run, after burn-in of 100 000 steps, for a total of 10 million steps per locus, to estimate parameters (see Methods S4 for complete Migrate settings). Migrate-N estimates the mutation-scaled effective population size $\theta = 4\ N_e \times \mu$, where N_e is the effective population size, and μ is the mutation rate per generation per locus, as well as mutation-scaled migration rate $M = m/\mu$, where m is the immigration

Table 1 Summary of population genetic parameters, over five variable loci, averaged in four regions along *Austrocedrus chilensis*'s range: Ch (Chile), Ar_N (north), Ar_C (central) and Ar_S (South) in Argentina (SE in parentheses)

Region	n	*A	*A_E	H_O	*H_E	*$P_{\%}$	*P_A	*P_T	Bn
Ch	7	7.09^{a} (0.84)	5.52^{a} (0.57)	0.70 (0.04)	0.70^{a} (0.01)	100^{ab}	1.11^{a} (0.25)	5.57^{a} (1.25)	0.156
Ar_N	12	5.73^{ab} (0.28)	4.16^{b} (0.27)	0.56 (0.03)	0.64^{ab} (0.02)	100^{b}	0.38^{b} (0.13)	1.92^{b} (0.63)	0.062
Ar_C	11	4.44^{bc} (0.29)	3.58^{b} (0.24)	0.61 (0.03)	0.59^{b} (0.02)	91^{a}	0.16^{b} (0.05)	0.82^{b} (0.26)	0.156
Ar_S	12	4.20^{c} (0.22)	3.21^{b} (0.20)	0.59 (0.04)	0.57^{b} (0.02)	92^{ab}	0.13^{b} (0.07)	0.67^{b} (0.36)	0.156
Grand mean (SE)		5.18 (0.25)	3.96 (0.19)	0.60 (0.02)	0.62 (0.01)	95.24 (1.33)	0.38 (0.08)	1.88^{b} (0.39)	

n, number of populations in the region; A, mean number of alleles per locus; A_E, mean number of effective alleles; H_O and H_E, observed and expected heterozygosity, respectively; $P_{\%}$, percentage of polymorphic loci; P_A, mean number of private alleles per locus; P_T, mean number of private alleles per population; *Bn*, *Bottleneck* probability of Wilcoxon one-tailed test for heterozygote excess under two-phase model of mutation. Statistically significant differences among regions (*, $P < 0.05$) in AMOVAs using GenAlEx with a 9999 permutations jackknifing procedure, (Peakall & Smouse, 2012), letters represent *post hoc* groupings after Bonferroni correction.

rate per generation among populations. We then calculated $N_e = \theta/4 \times \mu$. We estimated N_e using $\mu = 10^{-2}$ per locus per generation, as suggested by Udupa & Baum (2001) for nuclear microsatellites in a long-lived plant. To consider variability due to mutation rate assumption we also estimated N_e across a range of μ values (see Methods S5). R_{ST}-based migration rates (MR) and coalescence times (τ) were estimated following Slatkin (1995). We calculated the *average* coalescence time (TR) following Slatkin's equation 19 that assumes a radiation model where derived populations are currently isolated (no gene flow). The coalescence time *in generations* was calculated as $\tau = TR \times N_e$. We finally estimated the *absolute* coalescence time as $t = \tau \times$ average generation length. We calculated an average generation length for *Austrocedrus* of 50 yr from empirical data (Kitzberger, 1994, see Table S3).

Bottlenecks

Because population sizes differ along the *Austrocedrus* range, we used the program BOTTLENECK v1.2.02 (Piry *et al.*, 1999) to test for recent population bottlenecks. This program compares single population H_E with the predicted value for the observed number of alleles under the assumption of the mutation-drift equilibrium model (Ewens, 1972), generating a distribution through simulating the coalescent process under the two-phased model of mutation. We used a mode-shift indicator that allows the identification of populations that suffered recent bottlenecks from allele frequency data, and a one-tail Wilcoxon test to identify heterozygosity excess, which has been suggested as the best method to analyze < 20 loci (Luikart & Cornuet, 1998).

Results

SDM

The stepwise variable selection algorithm retained a final model with right contributing variables: BIO17 (precipitation of driest quarter, 26.4%), BIO4 (temperature seasonality, 25.4%), BIO13 (precipitation of wettest month, 15.0%), BIO11 (mean temperature of coldest quarter, 9.0%), BIO5 (maximum temperature of warmest month, 7.1%), BIO18 (precipitation of warmest quarter, 6.9%), BIO7 (temperature annual range, 5.1%), BIO15 (precipitation seasonality, 5.1%) (Fig. S2). Inclusion of other variables of the BioClim set increased training gain by < 1% of its previous value. The area under the curve of the final model across the five replicates was 0.981 + 0.002. Regularized training gain was 1.642 + 0.006. The 10th percentile of training sample logistic threshold (suitability threshold that contained 90% of training samples) was 0.550 + 0.011; this value was used as a threshold to divide high from low suitability areas for *Austrocedrus*, both for modern and LGM conditions. When the bioclimatic envelope was projected onto LGM conditions, clamping was zero throughout the study region for all five replicates, suggesting that modern spatial variability is a useful analog of LGM conditions. All of these results deliver credible suitability maps for *Austrocedrus*. SDMs show large changes in climatic suitability for *Austrocedrus* between full glacial and modern conditions (Figs 1, S3). Assuming that the 10th percentile training sample exclusion threshold divides suitable from unsuitable areas, *Austrocedrus* could have expanded its potential suitable range from full glacial to modern conditions by a factor of about five (Fig. S3). LGM refugia for the species would have been concentrated at mid-low latitudes (37–38°S), low altitudes (100–300 m above sea level, a.s.l.) and the western lower slopes of the Andes and Coastal Nahuelbuta range of Chile (Fig. S3). Only a small pocket (< 2%) of suitable range during LGM was located at *c.* 42° and within 50 km east of the Andean divide, at elevations below 400 m a.s.l. According to reconstructions of ice extent, these southern Argentine locations were covered by the ice sheet, so it is unlikely that they harbored refugial populations of *Austrocedrus* at LGM (Figs 1, S3). Furthermore, areas > 50 km east of the Andean divide, suggested by Pastorino & Gallo (2002) to have served as dry relict ice-free refugia, were strongly unsuitable for the species (Fig. S3). By contrast, modern suitable areas for the species are mostly distributed over an elongated region centered at *c.* 42°S and a less extensive region in the Chilean Andes, from 37 to 38°S. Interestingly the elevational range of currently suitable areas varies between *c.* 500 and 1300 m a.s.l. Suitable areas of the species have clearly shifted from more westerly lowland and low foothill locations in Chile to higher elevation eastern slopes, centered *c.* 25–60 km east of the continental divide in the dry ecotonal foothills, neighboring the Patagonian steppe (Fig. S3).

Genetic variation

No evidence for genotypic disequilibrium was found at any pair of loci (all $P > 0.05$), and neither was there a large allele dropout or detectable presence of nonamplifying alleles (null alleles). All five microsatellite loci were polymorphic and 79 out of 178 alleles were private (P_A), that is, present in a single population (Table S2).

Consistent with the hypothesis that genetic diversity decreases with increasing distance from the origin of expansion, within-population genetic diversity parameters decreased across the Andes (W → E↓) and then southwards (N → S↓). All five genetic diversity metrics were negatively and significantly ($P < 0.0001$) correlated with increasing latitude: ($r = -0.75$ for A), ($r = -0.71$ for A_E), ($r = -0.61$ for H_E), ($r = -40$ for $P_{\%}$) and ($r = -0.68$ for P_A) (Fig. 2). The Chilean regional cluster of populations attained significantly higher values of A, A_E, H_E, $P_{\%}$, P_A and P_T than the other population clusters (Table 1; Fig. 2).

Approximately half (39 of 79) of the private alleles appear in Chilean populations, where all populations have $P_A \geq 2$; the Chilean Andean populations showed the largest number of private alleles ($P_A = 26$). The number of private alleles, averaging seven, in Chilean Andean populations, decrease sharply eastward across the Andes, and south along the Cordillera, becoming one in Ar_S populations (Table S2). In keeping with the range expansion hypothesis, a cline in the mean frequency of shared alleles was observed along the range of *Austrocedrus* (Fig. 2).

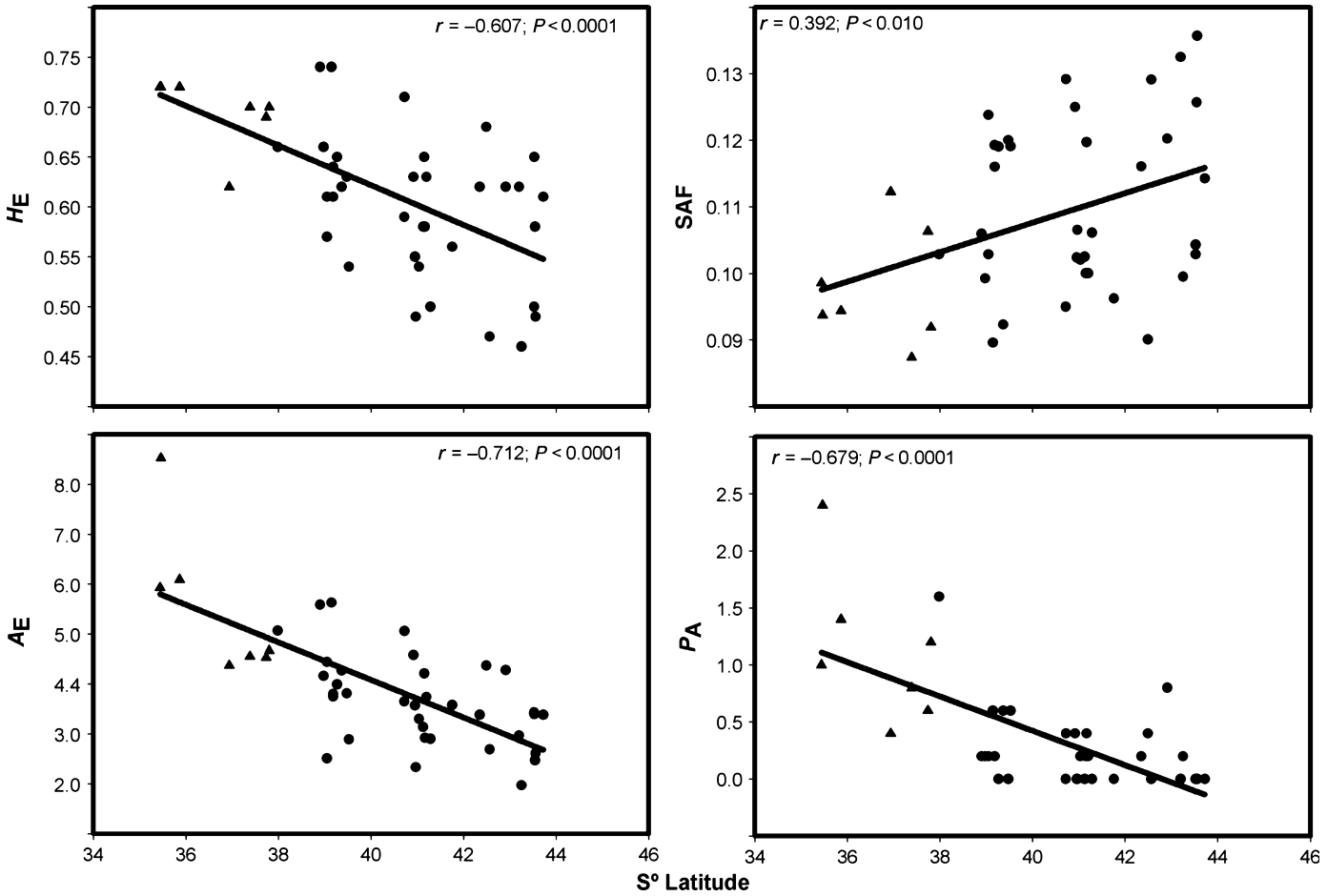

Fig. 2 Correlations between expected heterozygosity (H_E), mean number of effective alleles (A_E), mean frequency of shared alleles (SAF), and mean number of private alleles per locus (P_A) and latitude in 42 sampled populations of *Austrocedrus chilensis* along its range. Black triangles and circles indicate Chilean and Argentine populations, respectively.

Genetic inbreeding, divergence and structure

Average inbreeding within each of the 42 populations was high and positive ($F_{IS} > 0.175$), but only Argentinean northern populations had > 58% of all possible tests departing significantly from zero (Table S2). Chilean populations displayed the lowest degree of inbreeding ($F_{IS} < 0.099$). Out of a total of 200 possible tests, 19 were significant for departure from Hardy–Weinberg equilibrium (15 of 35 Argentine populations, and four of seven Chilean populations). Mean among-population divergence within regions by pairwise F_{ST} values ranged from 0 for pairs from Ar_N populations to 0.017 for pairs within the Ch group of populations. Overall genetic divergence, weighted over loci, among regions was significant but moderate $R_{ST} = 0.177$ (Tables 2, S4). A significant relationship between genetic and geographical distances was found in the Chilean region (Mantel test $r = 0.38$; $P = 0.04$, see later Fig. 4a), whereas a nonsignificant relationship was found in Argentine populations (Mantel test $r = 0.01$, $P = 0.41$, see later Fig. 4b). The relationship between genetic and geographic distances of the two areas differed significantly ($F_{1,619} = 18.5$, $P < 0.000$, homogenetiy of slopes test).

STRUCTURE analysis indicated that the overall genetic profile for *Austrocedrus* trees could be described with four genetic clusters, as reflected by both the highest likelihood value and a peak of ΔK detected at $K = 4$, that is, $\ln P(4) = -5900.83$, $\Delta K(4) = 10.10$ (Fig. S4; Table S5). These four genetic clusters are coincident with the main four natural geographic regions along the species' range (Ch, AR_N, AR_C, AR_S; Fig. 3). Bayesian assignment based on genetic similarities of individual trees to each of these four ancestral groups shows that 46% of trees from Ch belong to cluster 1, 64% of trees from Ar_N belong to cluster 2, 43% and 48% of trees from Ar_C belong to either cluster 3 or 4, and 58% of trees from Ar_S belong to cluster 4 (Fig. 3; Table S6). Most individuals were generally assigned with high probabilities to a single cluster, except for individuals from region Ar_C that could be equally assigned to either Ar_C or Ar_S, suggesting signals of admixture with individuals from Ar_S (Fig. 3). PCoA indicated four groups of populations, with the first three axes accounting for 80.94% of the genetic variation among 42 sampled populations (Fig. S5).

Effective population size, coalescence times and migration

Effective population sizes, derived from coalescent analysis, differ among regions ($155 < N_e < 265$), being greater in Chile

New Phytologist

Table 2 Mean effective population size scaled mutation rate (Θ) along with credibility intervals (CI 2.5–97.5%) and mean effective population size (N_e) in four regions along *Austrocedrus chilensis*'s range (Ch, Ar_N, Ar_C, Ar_S); these regions are also compared by pairwise genetic divergence (R_{ST}), coalescence time in generations (τ) and coalescence time in years (*t*)

			R_{ST}			τ (generations)			*t* (yr)		
Region	Θ	N_e	Ar_N	Ar_C	Ar_S	Ar_N	Ar_C	Ar_S	Ar_N	Ar_C	Ar_S
Ch	10.589 (6.333–15.667)	264.725	0.153*	0.400*	0.442*	178.5	560.2	702.4	8925	28 008	35 120
Ar_N	9.179 (5.400–14.667)	229.475	–	0.174*	0.196*	–	161.8	199.4	–	8089	9971
Ar_C	6.197 (3.200–9.133)	154.925		–	0.018*		–	11.9		–	594
Ar_S	7.131 (3.600–10.800)	178.275			–			–			–

Effective population size (N_e) was calculated based on Beerli & Felsenstein (2001), assuming a value of $\mu = 10^{-2}$, as suggested by Udupa & Baum (2001). See Supporting Information Methods S5 for alternative μ values. Average coalescence times (TR) were calculated based on Slatkin (1995), and the average generation time of *Austrocedrus* was calculated as 50 yr from Kitzberger (1994), see Table S3: $\tau = TR \times N_e$, with $TR = 4R_{ST}/(1 - R_{ST})$, and $t = \tau \times 50$ yr.
*Significantly different from 0.

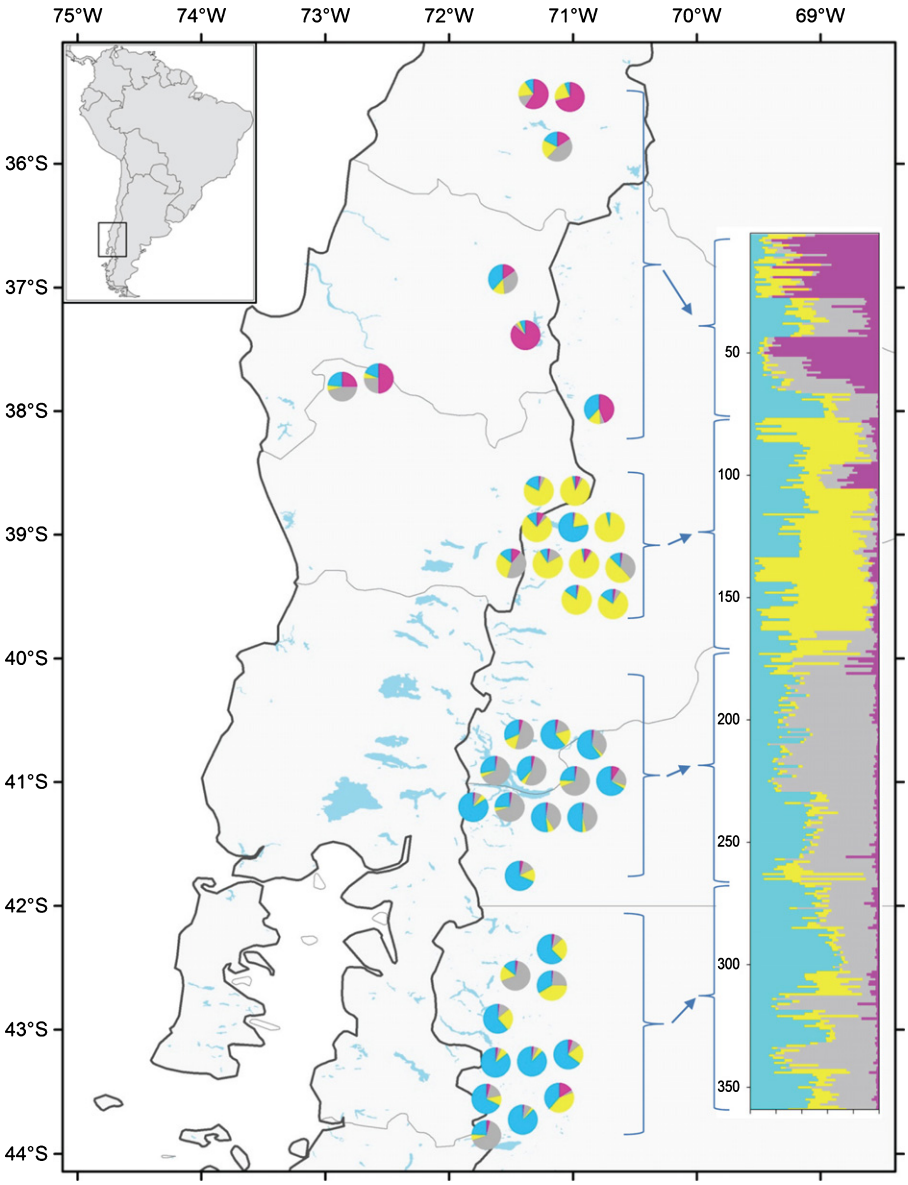

Fig. 3 Sampled sites of *Austrocedrus* and admixture genetic assignment of individuals based on Structure Bayesian clustering method. Pie charts represent the average coefficients of ancestry obtained at $K = 4$. In the right inset, Structure results as proportion of trees assigned to each cluster considering $K = 4$ in 42 populations. Colors represent different genotypic clusters: magenta, cluster 1; yellow, cluster 2; grey, cluster 3; turquoise, cluster 4.

(Table 2). As in genetic diversity results, N_e decreased sharply from Chilean populations, eastward across the Andes and southward towards central and southern Argentine populations (Fig. 4). Average coalescence times (τ) between each region and all remaining regions varied between 12 and 702 generations, being earlier for the Ch–Ar_S regions (Table 2). Coalescence time

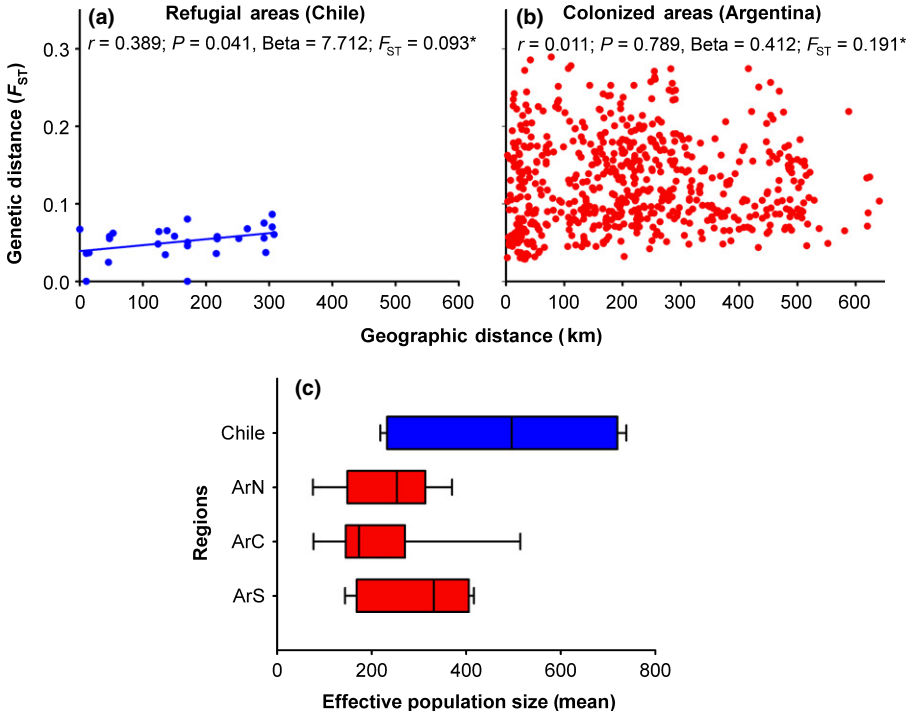

Fig. 4 Scatterplots of the genetic (F_{ST}) and geographical distances (km) within: (a) proposed Chilean refugia and (b) Argentine recolonized areas. Asterisks indicate significantly different from zero F_{ST} values. (c) Estimates of effective population size (N_e) based on mean individual locus values of Bayesian inferences in four *Austrocedrus* regions. The boundary of the box closest to zero indicates the 25th percentile, a line within the box marks the mean posterior values over individual loci, and the boundary of the box farthest from zero indicates the 75th percentile. Whiskers (error bars) above and below the box indicate the 90th and 10th percentiles.

in years (t) between Chile and Argentina is estimated as *c.* 14 kyr (Fig. 5).

Pairwise migration rates for $Ar_N \rightarrow Ar_C$, $Ar_N \rightarrow Ar_S$, $Ar_S \rightarrow Ar_C$ and $Ch \rightarrow Ar_N$ had higher support than the other pairs of regions (Table 3). Pairwise absolute coalescence times (t) reached their highest values of 35 kyr between Ch and Ar_S and 28 kyr between Ch and Ar_C (Table 2; Fig. 5). Within Argentina, the oldest relationship node is between regions Ar_N and Ar_S (10 kyr), with Bayesian support only in the N → S direction. A shorter coalescence time (8 kyr) was estimated for $Ar_N \rightarrow Ar_C$. Regions Ar_C and Ar_S have internal nodes as recent as *c.* 0.6 kyr, but with support in both directions. To assess whether the results are robust, we explored the influence of increasing mutation rate on estimated effective population size (N_e) and, consequently, on coalescence time (Methods S5). Evidently the Ch region always reached higher effective population size and that decreased sharply, eastward across the Andes and southward towards central and southern Argentina, supporting our results.

Bottlenecks

The analysis performed to infer bottlenecks under the two phase model indicated that in most *Austrocedrus* regions the observed gene diversity is not significantly higher than the expected equilibrium gene diversity (Wilcoxon tests, $P > 0.05$; BnWt P-values in Table 1). Only Ar_N populations showed marginally significant tests, suggesting recent bottlenecks in this region only.

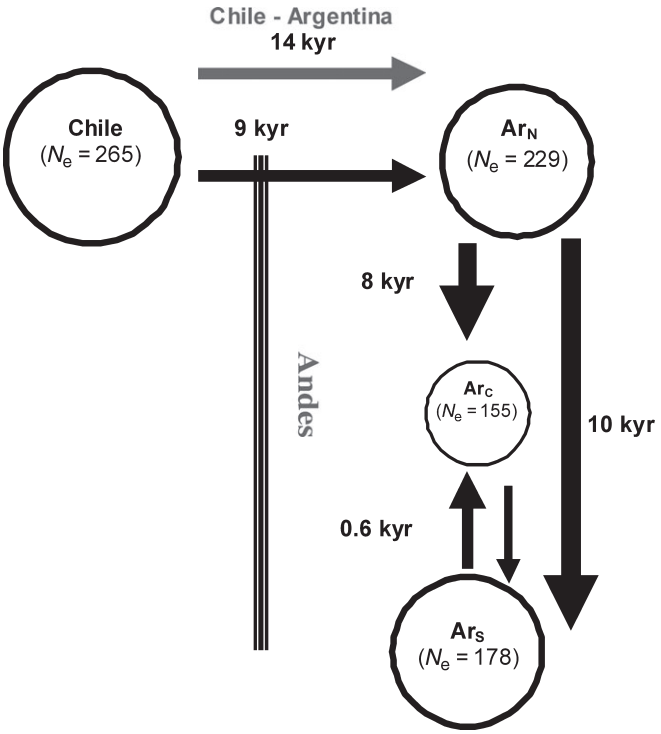

Fig. 5 Schematic representation of *Austrocedrus* migration estimated from MIGRATE. Arrows represent mean migration rates (M) among four regions along the *Austrocedrus* range. Absolute coalescence times (t) in brackets are given in thousand years (kyr) before present. Arrow thickness is proportional to M size. Balloon sizes are proportional to mean effective population sizes (N_e). Vertical line represents the Andes.

Discussion

Several scenarios have been postulated for how plant species respond to changing climate, and the evidence for such alternative responses can suggest different assessment of any species' potential to survive past, impending or even future climate changes (Pearson *et al.*, 2006). Paleoecological evidence suggests

Table 3 Pairwise MIGRATE parameters of migration (immigration rate scaled mutation rate, mean $M_{i\text{-}j}$) and credibility intervals (CI 2.5–97.5%), along with acceptance ratios from Bayesian analysis between region pairs through the *Austrocedrus* range

Pair of regions	$M_{i\text{-}j}$ (CI 2.5–97.5%)	Acceptance ratio
Ar_N–Ar_S	3.786 (0.0800–6.200)	0.11
Ar_N–Ar_C	3.777 (0.600–5.600)	0.12
Ar_S–Ch	3.178 (1.133–5.133)	0.11
Ar_C–Ch	3.080 (0.000–5.333)	0.11
Ar_S–Ar_C	2.749 (0.533–4.800)	0.11
Ch–Ar_N	2.477 (0.000–4.200)	0.10
Ar_S–Ar_N	2.375 (0.467–4.200)	*0.08*
Ch–Ar_C	2.351 (0.267–4.267)	0.11
Ch–Ar_S	2.222 (0.133–4.200)	0.10
Ar_C–Ar_N	1.946 (0.133–3.733)	*0.08*
Ar_C–Ar_S	1.764 (0.000–3.533)	0.10
Ar_N–Ch	1.457 (0.000–2.333)	0.13

Italics indicate low values of acceptance ratio.

that there are fast-tracking species (Petit *et al.*, 2008) and slow-tracking species (Birks, 1981; Svenning & Skov, 2004, 2007; McLachlan *et al.*, 2005).

In South American temperate forests, a suite of genetic studies suggest that relatively microthermic forest dominant genera (*Nothofagus*, *Fitzroya*, *Pilgerodendron*, *Podocarpus*, *Embothrium*) have been able to survive glacial periods locally (Sérsic *et al.*, 2011) in multiple ice-free refugia, rapidly recolonizing nearby areas (*sensu* Premoli, 1998). In addition, two groups of mesothermic tree species can be found: species of the Valdivian rainforest (genera *Eucryphia*, *Caldcluvia*, *Aextoxicon*), as well as drought-tolerant species occurring under some degree of water stress (*Austrocedrus*, *Araucaria*), the former typically outcompeted in high water availability conditions by *Nothofagus* species. Recent genetic surveys suggest that the Valdivian genera survived in northern refugial areas in the unglaciated Coastal Range of Chile (40°S for *Eucryphia*, and 32–39°S for *Aextoxicon*), expanding southward and eastwards into previously glaciated Andean areas in the early Holocene (Núñez-Ávila & Armesto, 2006; Segovia *et al.*, 2012). Despite warmer postglacial conditions, pollen records at 41–42°S show an absence of *Eucryphia*/*Caldcluvia* from *c.* 10 to 9 kyr BP, followed by a sudden increase (Moreno & León, 2003; Moreno, 2004), which lags behind the onset of Holocene warming and the appearance of cold-tolerant taxa by several millennia. The only genetic study on the mesothermic *Araucaria* comparing populations from Chile and Argentina showed that the most northerly populations on both slopes of the Andes were different from the most southerly Argentinean population and other southern-most Chilean populations (Bekessy *et al.*, 2002).

Our species distribution model shows that at the Last Glacial Maximum (LGM), *Austrocedrus* may have found suitable conditions along narrow elevation (120–240 m a.s.l.) and latitudinal belts of the west-facing foothills of the Chilean Coastal Range and the Andean Cordillera, within the Bio Bio Region in Chile (36–38°S; Figs 1a, S3). These areas show the highest levels of current genetic diversity within populations. They also provide evidence for a significant spatial genetic structure (SGS), with divergence among refugial populations suggesting long periods of isolation in areas located at the rear edge of the species' distribution, similar to the pattern suggested by Slatkin (1993). In accordance with range expansion theory (Slatkin, 1993), unique alleles and allelic diversity are highest in Chilean populations, decreasing sharply across the Andes into Argentina and steadily southwards. This creates an expected cline in the direction of the expansion front, because each founder event results in additional losses to genetic drift, yielding progressive losses of variation as species move from their initial source (refugial) populations.

A long-distance pattern is enforced by gradual genetic impoverishment with increasing latitude, suggesting successive founder events (Hewitt, 2000) resulting in impoverished genetic pools and a reduced SGS in the colonized area. Lack of identity-by-descent relationships in Argentine populations suggests that insufficient time has elapsed since range expansion to redevelop an internal SGS. Our results fit the pattern predicted by a model of progressive poleward erosion of genetic diversity (Hewitt, 2000). The SDM also suggests that the current range of *Austrocedrus*, across the Andes in Argentina, was largely unsuitable at the LGM (Fig. 1a). Following climate change conditions during the early Holocene, *Austrocedrus* may have been able to reach the elevations necessary to cross low Andean passes (Fig. S3). The southern advancement probably occurred in a wave-like fashion along the east Andean rain-shadow corridor between the mesic *Nothofagus* forests, which in turn rapidly expanded during the late glacial/early Holocene from local refugia (Premoli *et al.*, 2010) and the Patagonian steppe. Furthermore, migration models support an eastward trans-Andean/southward migration. Pairwise migration rates for $Ar_N \rightarrow Ar_C$, $Ar_N \rightarrow Ar_S$, $Ar_S \rightarrow Ar_C$ and Ch $\rightarrow Ar_N$ had higher support than between other possible pairs of regions and directions.

Because coalescence times describe the time it takes copies of a locus to find a common ancestor in the past, and therefore is nested within the history of the populations containing the sampled individuals and their ancestors, coalescence time is not the same as population splitting time. Coalescence times are often earlier than population splitting times, but the estimation of divergence time when gene flow occurs between the descendant populations after divergence can cause coalescence to occur more recently than divergence (Rosenberg & Feldman, 2002). In any case, for sufficiently large divergence times compared with populations sizes, if migration between populations is small, coalescence times are useful approximations for divergence times, and are typically somewhat correlated (Rosenberg & Feldman, 2002). This is probably the case for *Austrocedrus*'s postglacial migration history as reflected in progressive recolonization parameters (Tables 2, 3). We calculated the average coalescence time (TR) following eqn 19 of Slatkin (1995) that assumes a radiation model where derived populations are currently isolated (no gene flow). This model is particularly accurate for the Chilean–Argentine populations. In a previous manuscript (Souto *et al.*, 2012) we showed that the three regions within Argentina diverged during the Holocene, so we

are testing the Slatkin (1995) demographic model composed of two lineages (Chilean and Argentine populations) descending from a single common ancestor. This model is a simplification of our system and is especially accurate for the Chilean–Argentine regions pair, in which divergence values (R_{ST}) are almost twice those within Argentine populations. Moreover, the current west-dominant winds prevent the Argentine–Chilean gene flow via pollen. Also primary seed dispersal is highly limited (Kitzberger, 1994) –at most 100 m from the mother tree.

Coalescence time estimates between Chilean and Argentine *Austrocedrus* populations are debatable, particularly the mutation rate of nuclear microsatellite, because very few data are available in the literature regarding nuclear microsatellite mutation rates for plant species. Also, as shown in Fig. S3, environmental variation along the migration path might have affected among-population divergence times. Even considering variability in point estimates of divergence time calculated from the posterior distribution of Theta from MIGRATE or alternative mutation rates (Methods S5), it is clear that western Chilean populations showed higher effective population size values than Argentinean ones reflected in earlier divergence. This in combination with their higher genetic diversity strongly suggests that Chilean populations are the source of Argentine ones.

Moreover, our estimated dates of *Austrocedrus* trans-Andean migration between Chilean and northern Argentinean populations are consistent in magnitude and timing (17–7 kyr) with late glacial climatic changes across southern South America. These include distributions reconstructed from terrestrial taxa-independent proxies such as LGM ice sheet modeling (Hulton *et al.*, 2002) or ocean core sea surface temperature reconstruction (Kaiser *et al.*, 2005). *Austrocedrus* would have migrated to the eastern flanks of the Andes during the early Holocene, a timeframe supported by the presence of Cupressaceae pollen on the eastern slopes of the Andes 37–39°S by 11–10 kyr BP (Table S1). It is likely that gene flow between Chilean and northern Argentinean populations was relatively high during the early Holocene, as reflected by the absence of significant differences in several genetic parameters. A similar pattern was described for northern populations of the mesothermic *Araucaria* (Bekessy *et al.*, 2002). Larger genetic similarity between southern and central populations than between them and northern Argentine populations, however, suggests that migration south of 41°S may have occurred as a single event. This is consistent with low pollen percentages in early to mid-Holocene records of Cupressaceae followed by an abrupt increase between 6.4 and 5 kyr BP in numerous records between 40°57′S and 41°30′S (Table S1). We propose that this sudden increase in Cupressaceae pollen during the mid–late Holocene is related to the arrival and expansion of *Austrocedrus* into a region where it had been absent. This same pattern, but lagging by *c.* 2–3 kyr, is evident in pollen records located further south at *c.* 42°S, where sharp increases in Cupressaceae pollen occurred between 3.3 and 3.0 kyr BP, preceded by a near absence of such pollen at that latitude (Table S1).

A recently published (Iglesias *et al.*, 2012) record consisting of Cupressaceae pollen (10 kyr) from 42°20′S, apparently contradicts our Holocene migration hypothesis for *Austrocedrus* (Table S1). These authors interpreted the pollen record as presence of *Austrocedrus*, based on genetic evidence that suggests LGM survival within easterly refugia, located far out on rocky outcrops of the Argentine steppe (Pastorino & Gallo, 2002). This analysis and interpretation based on slightly higher levels of genetic variation within drier eastern (steppeward) populations compared with wetter Andean populations did not include Chilean samples, and therefore alternative hypotheses of refugial areas in Chile could not be tested.

Neither our species' distribution model nor our molecular data support the hypothesis of several small refugia located towards the steppe that may have served as sources of local expansion for extant Andean populations. First, retrodicted suitability for LGM suggests very harsh (cold) conditions for *Austrocedrus* survival in this area. Second, our geographic patterns of genetic impoverishment are progressively N → S not progressively E → W. Third, attempts to test hypotheses of E → W postglacial migration using MIGRATE Bayesian models resulted in lower effective population sizes for eastern ($\Theta_E = 0.03$) than for western ($\Theta_W = 11.57$) populations in Argentina along the 38–43°S belt, which further supports W → E expansion. Pairwise migration rates among populations had high Bayesian support, but were one order of magnitude larger from W to E ($M_{W \to E} = 13.05$) than in the reverse direction ($M_{E \to W} = 1.91$). More important, average coalescence times between eastern and western population groups within Argentina were a few generations long only, in stark contrast with millennial-scale coalescence times between Chilean and Argentinean groups.

Conclusion

The combined use of species distribution modeling, molecular and palynological evidence, as illustrated here, strongly suggests that cold-tolerant (microtherm) and cold-sensitive (mesotherm) taxa may have had different Holocene recolonization histories. In particular, Southern Hemisphere mesotherms have successfully coped with dramatic climatic change over extended time and space by occupying more northerly (climatically milder) refugia. This is the first comprehensive analysis of a drought-tolerant mesotherm tree species, showing alternative responses to past climatic changes, which highlight the importance of considering genecological tolerance to predict responses to future climate changes in keeping with species' differing constraints.

Acknowledgements

This research was carried out in the framework of the ReForLan project funded by the European Commission (FP6-2004-INCO-DEV-3 PROP no. 032132). C.P.S., T.K. and A.C.P. are members of CONICET. We thank Peter Smouse and two anonymous reviewers for their helpful comments that improved the quality of our manuscript.

References

Acosta MC, Mathiasen P, Premoli AC. 2014. Retracing the evolutionary history of *Nothofagus* in its geo-climatic context: new developments in the emerging field of phylogeology. *Geobiology* **12**: 497–510.

Allnutt TR, Newton AC, Lara A, Premoli AC, Vergara R, Gardner M. 1999. Genetic variation in *Fitzroya cupressoides* (alerce), a threatened South American conifer. *Molecular Ecology* **8**: 975–987.

Allnutt TR, Newton AC, Premoli AC, Lara A. 2003. Genetic variation in the threatened South American conifer *Pilgerodendron uviferum* (Cupressaceae), detected using RAPD markers. *Biological Conservation* **114**: 245–253.

Arana MV, Gallo LA, Vendramin GG, Pastorino MJ, Sebastiani F, Marchelli P. 2010. High genetic variation in marginal fragmented populations at extreme climatic conditions of the Patagonian Cypress *Austrocedrus chilensis*. *Molecular Phylogenetics and Evolution* **54**: 941–949.

Beerli P. 2002. *MIGRATE: documentation and program, part of LAMARC*. Seattle, WA, USA: Department of Genome Sciences, University of Washington.

Beerli P, Felsenstein J. 2001. Maximum likelihood estimation of a migration matrix and effective population sizes in n subpopulations by using a coalescent approach. *Proceedings of the National Academy of Sciences, USA* **98**: 4563–4568.

Beerli P, Palczewski M. 2010. Unified framework to evaluate panmixia and migration direction among multiple sampling locations. *Genetics* **185**: 313–326.

Bekessy SA, Allnutt TR, Premoli AC, Lara A, Ennos RA, Burgman MA, Cortes M, Newton AC. 2002. Genetic variation in the vulnerable and endemic monkey puzzle tree, detected using RAPDs. *Heredity* **88**: 243–249.

Birks HJB. 1981. The use of pollen analysis in the reconstruction of past climates: a review. In: Slatkin M, Veuille M, eds. *Climate and history*. Oxford, UK: Oxford University Press, 111–138.

Bran D, Pérez A, Barrios D, Pastorino MJ, Ayesa J. 2002. *Eco-región Valdiviana: Distribución actual de los bosques de "Ciprés de la Cordillera" (Austrocedrus chilensis) Escala 1:250.000*. Bariloche, Argentina: INTA, APN, FVSA.

Collins WD, Bitz CM, Blackmon ML, Bonan GB, Bretherton CS, Carton JA, Chang P, Doney SC, Hack JJ, Henderson TB *et al.* 2006. The community climate system model: CCSM3. *Journal of Climate* **19**: 2122–2143.

CONAF (Corporación Nacional Forestal), CONAMA (Comisión Nacional del Medio Ambiente), BIRF (US Bank International Reconstruction Fomentation). 1999. *Chilean National report including environmental variables. Catastro y evaluación de los recursos vegetacionales nativos de Chile*. Santiago, Chile: CONAF.

Débarre F, Ronce O, Gandon S. 2013. Quantifying the effects of migration and mutation on adaptation and demography in spatially heterogeneous environments. *Journal of Evolutionary Biology* **26**: 1185–1202.

Dezzotti A, Sancholuz L. 1991. Los bosques de *Austrocedrus chilensis* en Argentina: ubicación, estructura y crecimiento. *Bosque* **12**: 43–52.

Donoso C. 1982. Reseña ecológica de los bosques mediterráneos de Chile. *Bosque* **4**: 117–146.

Doyle JJ. 1990. Isolation of plant DNA from fresh tissue. *Focus* **12**: 13–15.

Dumolin S, Demesure B, Petit RJ. 1995. Inheritance of chloroplast and mitochondrial genomes in pedunculate oak investigated with an efficient PCR method. *Theoretical and Applied Genetics* **91**: 1253–1256.

Ewens WJ. 1972. The sampling theory of selectively neutral alleles. *Theoretical Population Biology* **3**: 87–112.

Gavin DG, Fitzpatrick MC, Gugger PF, Heath KD, Rodríguez-Sánchez F, Dobrowski SZ, Hampe A, Hu Feng S, Ashcroft MB, Bartlein PJ *et al.* 2014. Climate refugia: joint inference from fossil records, species distribution models and phylogeography. *New Phytologist* **204**: 37–54.

Gilbert KJ, Andrew RL, Bock DG, Franklin MT, Kane NC, Moore JS, Moyers BT, Renaut S, Rennison DJ, Veen T *et al.* 2012. Recommendations for utilizing and reporting population genetic analyses: the reproducibility of genetic clustering using the program structure. *Molecular Ecology* **21**: 4925–4930.

Goodman SJ. 1997. RST Calc: a collection of computer programs for calculating estimates of genetic differentiation from microsatellite data and determining their significance. *Molecular Ecology* **6**: 881–885.

Goudet J. 2000. *FSTAT. A program to estimate and test gene diversities and fixation indices. Version 2.9.1*. Dorigny, Switzerland: Université de Lausanne.

Hampe A, Rodríguez-Sánchez F, Dobrowski S, Hu FS, Gavin DG. 2013. Climate refugia: from the Last Glacial Maximum to the twenty-first century. *New Phytologist* **197**: 16–18.

Hewitt GM. 2000. The genetic legacy of the Quaternary ice ages. *Nature* **405**: 907–913.

Hijmans RJ, Cameron S, Parra J, Jones PG, Jarvis A. 2005. WorldClim – global climate data. Very high resolution interpolated climate surfaces for global land areas. *International Journal of Climatology* **25**: 1965–1978.

Hu FS, Hampe A, Petit RJ. 2009. Paleoecology meets genetics: deciphering past vegetational dynamics. *Frontiers in Ecology and the Environment* **7**: 371–379.

Hulton NRJ, Purves RS, McCulloch RD, Sugden DE, Bentley MJ. 2002. The last glacial maximum and deglaciation in southern South America. *Quaternary Science Reviews* **21**: 233–241.

Iglesias V, Whitlock C, Bianchi MM, Villarosa G, Outes V. 2012. Holocene climate variability and environmental history at the Patagonian forest/steppe ecotone: Lago Mosquito. 42.50°S, 71.40°W) and Laguna del Cóndor (42.20°S, 71.17°W). *The Holocene* **22**: 1297–1307.

INTA, APN, UACh, FVSA y WWF. 1999. Mapeo de la Eco-región de los Bosques Valdivianos: Informe Final, Escala 1:500.000. *Boletín Técnico Fundación Vida Silvestre* **51**: 1–27.

IUCN. 2014. *Red List of Threatened Species. Version 2014.3*. International Union for the Conservation of Nature. [WWW document] URL www.iucnredlist.org [accessed 8 May 2015].

Kaiser J, Lamy F, Hebbeln D. 2005. A 70-kyr sea surface temperature record off southern Chile (Ocean Drilling Program Site 1233). *Paleoceanography* **20**: PA4009.

Kitzberger T. 1994. *Fire regime variation along a northern Patagonian forest-steppe gradient: stand and landscape response*. PhD thesis, University of Colorado, Boulder, CO, USA.

Luikart G, Cornuet JM. 1998. Empirical evaluation of a test for identifying recently bottlenecked populations from allele frequency data. *Conservation Biology* **12**: 228–237.

Markgraf V, D'Antoni HL, Ager TA. 1981. Modern pollen dispersal in Argentina. *Palynology* **5**: 43–63.

Markgraf V, Iglesias V, Whitlock C. 2013. Late and postglacial vegetation and fire history from Cordón Serrucho Norte, northern Patagonia. *Palaeogeography, Palaeoclimatology, Palaeoecology* **371**: 109–118.

Markgraf V, McGlone M, Hope G. 1995. Neogene paleoenvironmental and paleoclimatic change in southern temperate ecosystems – a southern perspective. *Trends in Ecology and Evolution* **10**: 143–147.

Mathiasen P, Premoli AC. 2010. Out in the cold: genetic variation of *Nothofagus pumilio* (Nothofagaceae) provides evidence for latitudinally distinct evolutionary histories in austral South America. *Molecular Ecology* **19**: 371–385.

McLachlan JS, Clark JS, Manos PS. 2005. Molecular indicators of tree migration capacity under rapid climate change. *Ecology* **86**: 2088–2098.

Moreno PI. 2004. Millennial-scale climate variability in northwest Patagonia over the last 15000 yr. *Journal of Quaternary Science* **19**: 35–47.

Moreno PI, León AL. 2003. Abrupt vegetation changes during the last glacial to Holocene transition in mid-latitude South America. *Journal of Quaternary Science* **18**: 787–800.

Nogués-Bravo D. 2009. Predicting the past distribution of species climatic niches. *Global Ecology and Biogeography* **18**: 521–531.

Normand S, Ricklefs RE, Skov F, Bladt J, Tackenberg O, Svenning JC. 2011. Postglacial migration supplements climate in determining plant species ranges in Europe. *Proceedings of the Royal Society B* **278**: 3644–3653.

Núñez-Ávila MC, Armesto JJ. 2006. Relict islands of the temperate rainforest tree *Aextoxicon punctatum* (Aextoxicaceae) in semi-arid Chile: genetic diversity and biogeographic history. *Australian Journal of Botany* **54**: 733–743.

van Oosterhout C, Hutchinson WF, Wills DP, Shipley P. 2004. Micro-checker: software for identifying and correcting genotyping errors in microsatellite data. *Molecular Ecology Notes* **4**: 535–538.

Ortego J, Riordan EC, Gugger PF, Sork VL. 2012. Influence of environmental heterogeneity on genetic diversity and structure in an endemic southern Californian oak. *Molecular Ecology* **21**: 3210–3223.

Pastorino MJ, Gallo LA. 2002. Quaternary evolutionary history of *Austrocedrus chilensis*, a cypress native to the Andean-Patagonian forest. *Journal of Biogeography* **29**: 1167–1178.

Peakall R, Smouse PE. 2006. GENALEX 6: genetic analysis in Excel. Population genetic software for teaching and research. *Molecular Ecology Notes* **6**: 288–295.

Peakall R, Smouse PE. 2012. GenAlEx 6.5: genetic analysis in Excel. Population genetic software for teaching and research-an update. *Bioinformatics* **28**: 2537–2539.

Pearson RG, Thuiller W, Araújo MB, Martinez-Meyer E, Brotons L, McClean C, Miles L, Segurado P, Dawson TP, Lees DC. 2006. Model-based uncertainty in species range prediction. *Journal of Biogeography* **33**: 1704–1711.

Petit RJ, Hu FS, Dick CW. 2008. Forests of the past: a window to future changes. *Science* **320**: 1450–1452.

Phillips SJ, Anderson RP, Schapire RE. 2006. Maximum entropy modeling of species geographic distributions. *Ecological Modelling* **190**: 231–259.

Piry S, Luikart G, Cornuet JM. 1999. Computer note. BOTTLENECK: a computer program for detecting recent reductions in the effective size using allele frequency data. *Journal of Heredity* **90**: 502–503.

Premoli AC. 1997. Genetic variation in a geographically restricted and two widespread species of South American Nothofagus. *Journal of Biogeography* **24**: 883–892.

Premoli AC. 1998. Use of genetic markers to conserve endangered species and to design protected areas for more widespread species. In: International Foundation for Science (eds). *Proceedings of International Workshop on Recent Advances in Biotechnology for Tree Conservation and Management* Santa Catarina, Brazil: Universidade Federal de Santa Catarina., 157–171.

Premoli AC, Kitzberger T, Veblen TT. 2000. Isozyme variation and recent biogeographical history of the long-lived conifer *Fitzroya cupressoides*. *Journal of Biogeography* **27**: 251–260.

Premoli AC, Mathiasen P, Kitzberger T. 2010. Southern-most *Nothofagus* trees enduring ice ages: genetic evidence and ecological niche retrodiction reveal high latitude (54°S) glacial refugia. *Palaeogeography, Palaeoclimatology, Palaeoecology* **298**: 247–256.

Premoli AC, Souto CP, Rovere AE, Allnut TR, Newton AC. 2002. Patterns of isozyme variation as indicators of biogeographic history in *Pilgerodendron uviferum* (D. Don) Florín. *Diversity and Distributions* **8**: 57–66.

Premoli AC, Souto C, Rovere A, Allnutt TR, Newton AC. 2001. Patterns of isozyme variation as indicators of biogeographic history in *Pilgerodendron uviferum*. *Diversity & Distribution* **8**: 57–66.

Pritchard JK, Stephens M, Donnelly P. 2000. Inference of population structure using multilocus genotype data. *Genetics* **155**: 945–959.

Quiroga MP, Premoli AC. 2010. Genetic structure of *Podocarpus nubigena* (Podocarpaceae) provides evidence of Quaternary and ancient historical events. *Palaeogeography, Palaeoclimatology, Palaeoecology* **285**: 186–193.

Rosenberg NA, Feldman MW. 2002. The relationship between coalescence times and population divergence times. In: Slatkin M, Veuille M, eds. *Modern developments in theoretical population genetics: the legacy of Gustave Malécot*. Oxford, UK: Oxford University Press, 130–164.

Rousset F. 1996. Equilibrium values of measures of population subdivision for stepwise mutation processes. *Genetics* **142**: 1357–1362.

Segovia RA, Pérez MF, Hinojosa LF. 2012. Genetic evidence for glacial refugia of the temperate tree *Eucryphia cordifolia* (Cunoniaceae) in southern South America. *American Journal of Botany* **99**: 121–129.

Seibert P. 1972. The structure of some forest communities in the Southern Cordillera (Argentina). *Forstwissenschaftliches Centralblatt* **91**: 278–291.

Sérsic AN, Cosacov A, Cocucci AA, Johnson LA, Pozner R, Avila lJ, Sites JW, Morando M. 2011. Emerging phylogeographical patterns of plants and terrestrial vertebrates from Patagonia. *Biological Journal of the Linnean Society* **103**: 475–494.

Slatkin M. 1993. Isolation by distance in equilibrium and nonequilibrium populations. *Evolution* **47**: 264–279.

Slatkin M. 1995. A measure of population subdivision based on microsatellite allele frequencies. *Genetics* **139**: 457–462.

Slatkin M, Excoffier L. 2012. Serial founder effects during range expansion: a spatial analog of genetic drift. *Genetics* **191**: 171–181.

Smith WHF, Sandwell DT. 1997. Global seafloor topography from satellite altimetry and ship depth soundings. *Science* **277**: 1956–1962.

Souto CP, Heinemann K, Kitzberger T, Newton AC. 2012. Genetic diversity and structure in *Austrocedrus chilensis* populations: implications for dryland forest restoration. *Restoration Ecology* **20**: 568–575.

Souto CP, Premoli AC. 2008. Genetic variation in the widespread *Embothrium coccineum* (Proteaceae) endemic to Patagonia: effects of phylogeny and historical events. *Australian Journal of Botany* **55**: 809–817.

Svenning JC, Skov F. 2004. Limited filling of the potential range in European tree species. *Ecology Letters* 7: 565–573.

Svenning JC, Skov F. 2007. Could the tree diversity pattern in Europe be generated by postglacial dispersal limitation? *Ecology Letters* **10**: 453–460.

Udupa SM, Baum M. 2001. High mutation rate and mutational bias at (TAA) n microsatellite loci in chickpea (*Cicer arietinum* L.). *Molecular Genetics and Genomics* **265**: 1097–1103.

Veblen TT, Burns BR, Kitzberger T, Villalba R. 1995. The ecology of the conifers of southern South America. In: Enright NJ, Hill RS, eds. *Ecology of the southern conifers*. Melbourne, Vic., Australia: Melbourne University Press, 120–155.

Veblen TT, Schlegel FM. 1982. Reseña ecológica de los bosques del sur de Chile. *Bosque* **4**: 73–115.

Vidal-Russell R, Souto CP, Premoli AC. 2011. Multiple Pleistocene refugia in the widespread Patagonian tree Embothrium coccineum (Proteaceae). *Australian Journal of Botany* **59**: 299–314.

Supporting Information

Additional supporting information may be found in the online version of this article.

Fig. S1 Model extent with training points.

Fig. S2 Model training gain with stepwise removal of variables.

Fig. S3 Refugia/suitable areas for *Austrocedrus* as a function of latitude, elevation and E–W distance to the Andean continental divide.

Fig. S4 STRUCTURE results.

Fig. S5 Principal coordinate analysis.

Table S1 Palynological evidence of Cupressaceae temporal patterns

Table S2 Geographic location and summary of population genetic parameters

Table S3 Average generation time for *Austrocedrus*

Table S4 *F* statistics

Table S5 STRUCTURE results, number of clusters (*K*)

Table S6 STRUCTURE average coefficients of ancestry (*Q*)

Methods S1 DNA extraction method, microsatellite primers and PCR conditions.

Methods S2 MAXENT methods, control parameters and settings.

Methods S3 STRUCTURE detail methods, parameters and settings.

Methods S4 MIGRATE parameters.

Methods S5 Extended MIGRATE results.

Please note: Wiley Blackwell are not responsible for the content or functionality of any supporting information supplied by the authors. Any queries (other than missing material) should be directed to the *New Phytologist* Central Office.